

RAPID COMMUNICATION

Differential Regulation of Synaptic Plasticity of the Hippocampal and the Hypothalamic Inputs to the Anterior Thalamus

Marian Tsanov,^{1,2} Seralynne D. Vann,³ Jonathan T. Erichsen,⁴ Nick Wright,⁴ John P. Aggleton,³ and Shane M. O'Mara^{1,2*}

ABSTRACT: The hippocampus projects to the anterior thalamic nuclei both directly and indirectly via the mammillary bodies, but little is known about the electrophysiological properties of these convergent pathways. Here we demonstrate, for the first time, the presence of long-term plasticity in anterior thalamic nuclei synapses in response to high- and low-frequency stimulation (LFS) in urethane-anesthetized rats. We compared the synaptic changes evoked via the direct vs. the indirect hippocampal pathways to the anterior thalamus, and found that long-term potentiation (LTP) of the thalamic field response is induced predominantly through the direct hippocampal projections. Furthermore, we have estimated that long-term depression (LTD) can be induced only after stimulation of the indirect connections carried by the mammillothalamic tract. Interestingly, basal synaptic transmission mediated by the mammillothalamic tract undergoes use-dependent, BDNF-mediated potentiation, revealing a distinct form of plasticity specific to the diencephalic region. Our data indicate that the thalamus does not passively relay incoming information, but rather acts as a synaptic network, where the ability to integrate hippocampal and mammillary body inputs is dynamically modified as a result of previous activity in the circuit. The complementary properties of these two parallel pathways upon anterior thalamic activity reveal that they do not have duplicate functions. © 2009 Wiley-Liss, Inc.

KEY WORDS: anterior thalamic nuclei; fornix; mammillothalamic tract; subiculum; LTP

INTRODUCTION

The hippocampus and anterior thalamic nuclei form key components of a neural circuit linking medial temporal lobe and medial diencephalic regions required for episodic memory (Aggleton and Brown, 1999; Warburton et al., 2001). Within this circuit, anterior ventral and anterior medial thalamic nuclei both receive: (i) direct inputs from the hippocampus (subiculum) via the fornix, and (ii) indirect hippocampal (subicular) inputs from the medial mammillary bodies via the mammillothala-

mic tract (Meibach and Siegel, 1975; Aggleton et al., 1986; Ishizuka, 2001). Although hippocampal projections to the mammillary bodies and anterior thalamic nuclei originate from the same regions of subiculum, they arise from separate neuronal populations (Ishizuka, 2001). The importance of the mammillothalamic tract for memory is emphasized by the repeated finding that damage to this tract is characteristic of thalamic strokes, which induce amnesia (von Cramon et al., 1985; Van der Werf et al., 2003). Current models of how the convergent inputs to the anterior thalamic circuitry might support memory emphasize the flow of hippocampal information through these pathways without explaining how these relays might transform or modulate this information in a way vital for memory. Both synaptic and nonsynaptic mechanisms of neuronal plasticity underpin experience-dependent alterations in brain networks and hypothetically at least, support long-term memory processes (Madison et al., 1991; Moser et al., 1998). The present study, therefore, compared activity-dependent plasticity within the anterior thalamic nuclei (Fig. 1A, inset), following stimulation of either the dorsal fornix (Dfx, Fig. 1B) or the mammillothalamic tract (MTT). Our first goal was to determine whether LTP or LTD can be induced in the separate anterior thalamic nuclei inputs.

To examine basal mammillothalamic synaptic transmission, animals underwent implantation of bipolar stimulating electrodes in MTT and a recording electrode in the ipsilateral anterior ventral thalamic nucleus (Fig. 1A). Male 7- to 10-week-old Lister-Hooded rats (Harlan, UK) were triple housed and maintained on 12:12 h light:dark cycles with food and water provided ad libitum. Under urethane anesthesia (ethyl carbamate: 1.5 g/kg, i.p.), the animals underwent insertion of a monopolar recording electrode (RNEX-300, David Kopf Instruments Ltd.) in the anterior thalamic nuclei (Fig. 1C) and bipolar stimulating electrodes in the mammillothalamic tract (MMT) (Fig. 1D). For the recording electrode, a drill hole was made in the cranium (1 mm in diameter), 1.1–1.3 mm posterior to bregma and 1.4–1.6 mm lateral to the midline, dorsal to the anterior ventral thalamic nucleus (ATN) in the rat (Krugeter et al., 1995).

¹ Trinity College Institute of Neuroscience, Trinity College Dublin, Ireland; ² School of Psychology, Trinity College Dublin, Ireland; ³ School of Psychology, Cardiff University, United Kingdom; ⁴ School of Optometry and Vision Sciences, Cardiff University, United Kingdom
Grant sponsor: Wellcome Trust (to J.P.A. and S.M.O'M); Grant number: W01048.

*Correspondence to: Shane M. O'Mara, Trinity College Institute of Neuroscience, Trinity College Dublin, Dublin 2, Ireland.
E-mail: smomara@tcd.ie

Accepted for publication 23 October 2009

DOI 10.1002/hipo.20749

Published online 30 December 2009 in Wiley Online Library (wileyonlinelibrary.com).

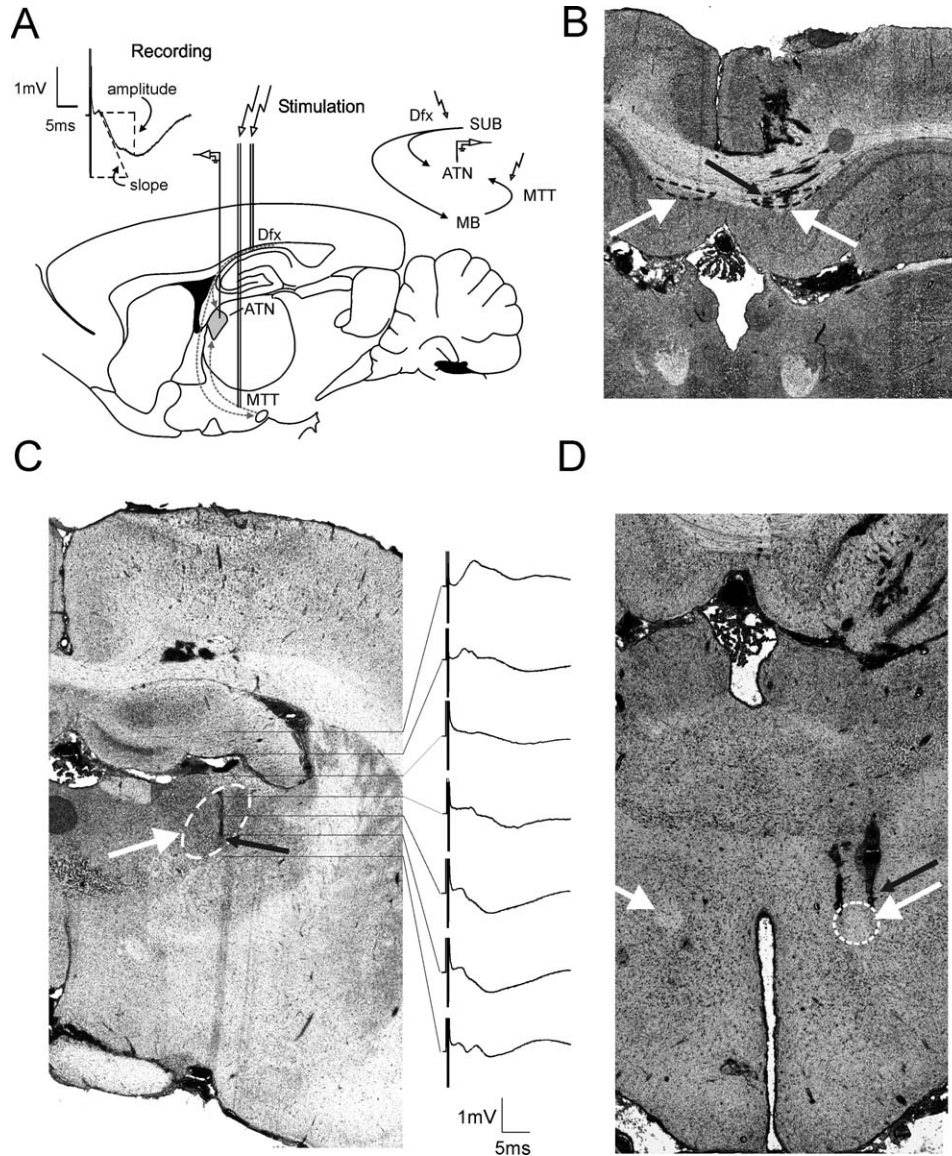


FIGURE 1. Experimental design for plasticity-inducing recordings in anterior thalamic nuclei of anesthetized animals. (A) Illustration of the position of the bipolar stimulating electrodes in dorsal fornix (Dfx) and mammillothalamic tract (MTT), and monopolar recording electrode in the ventral anterior thalamic nucleus (ATN). The circuitry of hippocampodienecephalic connections, schematically represented in the upper right corner, reveals the parallel hippocampal outputs. Stimulation of Dfx allows slope measurement of monosynaptic onset recording from ATN, shown as the upper left inset, while the stimulation of MTT represents the indirect pathway passing through the mammillary bodies (MB). (B) Coronal section showing stimulating electrode tracks

that reach Dfx. (C) Coronal section revealing the track of recording electrode in ATN. The column on right shows field potentials recorded at different depths in response to MTT stimulation. Each step, marked with the horizontal lines, represents 400 μ m. Horizontal bar: 5 ms, vertical bar 1 mV. (D) The stimulation electrodes were alternatively positioned in MTT; the histological section shows stimulation electrode tracks reaching MTT. White arrows point to the targeted structures in (C) and (D) (marked with dashed line) ipsilateral to the recording site; contralateral fiber tracts are also noted. Smaller black arrows point to the location of electrode tips.

A recording electrode was lowered 5.0 mm from the dural surface to reach ATN. A second drill hole was made for a bipolar stimulating electrode with coordinates targeting MTT (2.3–2.5 mm posterior to bregma, 0.8–1.0 mm lateral to midline). Alternatively, for the experiments that monitored the direct hippocampothalamic connection, the stimulation electrodes were positioned for Dfx coordinates (3.3–3.5 mm posterior to

bregma, 0.3–0.5 mm lateral to midline) (Fig. 1B). A stimulating electrode was positioned in the MTT/Dfx ipsilateral to the hemisphere from which ATN recordings were obtained. The depth was 5.0–6.0 mm from the dural surface for MTT and 1.5–2.5 mm for Dfx (Kruger et al., 1995). Final positions of the stimulating and recording electrodes were then determined by maximizing the amplitude of the field potential recorded in

the ATN in response to electrical stimulation of MTT/Dfx. Monopolar recordings from ATN were made relative to ground and reference screws inserted into the contralateral parietal and frontal bones. Once verification of the location of the electrodes was complete, recordings were allowed to stabilize for 10 min before experiment.

Signals were filtered between 0.1 Hz and 1 kHz, and then amplified (DAM-50 differential amplifier; World Precision Instruments, Hertfordshire, UK). Recordings were digitized online using a PC connected to a CED-1401 plus interface and analyzed using Spike 2 software (CED, Cambridge, UK). Field potential (FP) slope and amplitude were used as a measure of excitatory synaptic transmission in the ATN region. To obtain these measurements, an evoked response was generated in Dfx or MTT by stimulating at low frequency (0.025 Hz) with single biphasic square wave pulses of 0.1 ms duration per half wave, generated by a constant current isolation unit. For each time point measured during the experiments, five records of evoked responses were averaged. The FP slope was measured as the intermediate 90% of the slope value between the first positive and the first negative deflections of the FP. The FP amplitude represents the absolute difference between the value of the first positive and the value of the first negative deflections of the FP (Fig. 1A, up-left inset). In addition, we measured the FP maximal slope through the five steepest points obtained on the negative deflection of the FP. The latency of the field potential was measured in milliseconds from the first positive deflection to the maximal point of the negative deflection. By means of input-output (IO) curve determination, the maximum FP was found, and during experiments, all potentials used as baseline criteria were evoked at a stimulus intensity that produced 40% of this maximum (100–400 μ A). The baseline FP data were obtained by averaging the response to stimulation of the MTT/Dfx, to obtain five sweeps at 40 s intervals, every 5 min over a period of 30 min. Electrophysiological data were then expressed as the mean percentage of baseline FP \pm standard error of the mean (S.E.M.). Statistical significance was estimated by using factorial analysis of variance (ANOVA). Using a factorial ANOVA, we estimated the effects of the stimulation protocol and the effect of time on the field potential values compared with the baseline period, composed of the first six time points. The probability level interpreted as statistically significant was $P < 0.05$.

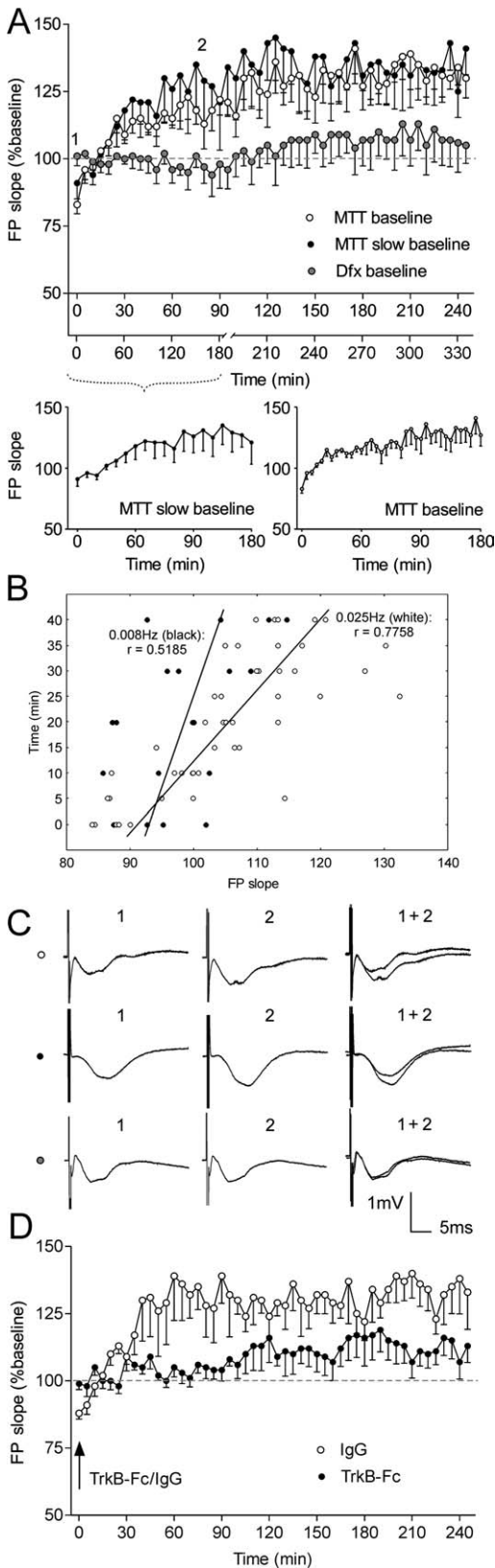
During baseline test-pulse stimulation, the MTT-evoked FP slope and amplitude gradually increased their values within the first 30 min of the recordings. Consistently, for all the animals in this group, the FP slope reached 130–160% of the first recorded value for each experiment (Fig. 2A, $n = 5$). The same change was evident for the FP amplitude (data not shown), although both parameters did not always share the same percentage increase when compared with individual recordings. In comparison with MTT stimulation, Dfx baseline recordings had a different profile. The average baseline for Dfx test-pulses did not show long-term alteration of the FP slope (Fig. 2A, $n = 4$) and amplitude (data not shown). In this case the ATN FP was evoked predominantly via the direct projections as the

low amplitude of the evoked response was not enough to induce a population spike response in MMB and subsequent transsynaptic activation of ATN through MMB. The restricted nature of the synaptic transmission is supported by the monosynaptic latency of the Dfx-evoked FP onset (2–3 ms), which determines the slope measurement in our recordings (Fig. 1A).

Our next experiment was designed to identify the trigger for mammillothalamic baseline augmentation. One of the most common models of homosynaptic plasticity proposes the rate of synaptic activation as a major factor in Hebbian modifications (Bienenstock et al., 1982). Neuronal stimulation with a frequency of less than 0.1 Hz is usually regarded as having no effect on the plasticity of hippocampal and cortical synaptic transmission (Lisman, 1994). We therefore used test pulses with a rate of 0.025 Hz to evoke baseline neuronal responses before the application of plasticity-inducing stimulation protocols. Recent findings, however, show that thalamocortical responses in vivo recorded with a baseline frequency of 0.025 Hz can undergo activity-dependent potentiation per se (Tsanov and Manahan-Vaughan, 2007a). In order to distinguish the role of baseline test-pulse rate as a factor in the observed phenomenon, we recorded mammillothalamic synaptic transmission with a baseline frequency lower than 0.025 Hz. The test-pulses for this group of animals were given every 120 s (0.008 Hz), monitored for 3 h (slow baseline) and then reset back to 0.025 Hz for another 2.5 h for the rest of the experiment. If the FP augmentation is frequency-driven, then the increase of the thalamic response in this group would be expected to be diminished or absent. Interestingly, the baseline synaptic transmission profile (Fig. 2A) appeared to reach the same amplitude as in the 0.025 Hz frequency group. The FP slope increased during the first 10 time points, showing no significant difference from the 0.025 Hz frequency group, when the data are compared on equalized time scale (Fig. 2A, ANOVA, $F < 1$, $P = 0.903$, $n = 5$). A similar pattern was observed for FP amplitude (ANOVA, $F < 1$, $P = 0.810$, $n = 5$, data not shown), where the potentiation dynamics were not time-related but appeared to be dependent on the number of pulses delivered to MTT. Analyzing the data of the first 10 time points with the original time scales for 0.008 Hz (Fig. 2A inset below-left) and 0.025 Hz baseline (Fig. 2A inset below-right), we find a significant difference in the pattern of FP augmentation (ANOVA, $F_{(1,9)} = 4.02$, $P < 0.05$, $n = 5$). This pattern can be presented also as different correlations between the slope values and time points for each frequency (Pearson's, $r = 0.5185$ for 0.008 Hz and $r = 0.7758$ for 0.025 Hz, Fig. 2B).

A challenging issue was to explore the mechanism responsible for the pulse-dependent increase of the mammillothalamic responses. Two related pieces of evidence were considered in our investigation: (1) anterior ventral thalamic nucleus possesses substantial fiber/terminal BDNF-immunoreactivity (Conner et al., 1997; Snyder et al., 1997) and (2) exogenous application of BDNF can induce a rapid and persistent enhancement of synaptic transmission in hippocampal and cortical preparations (Kang and Schuman, 1995; Akaneya et al., 1997). Application of BDNF induces a slow-onset, persistent strengthening of syn-

aptic transmission at hippocampal synapses in vivo (Messaoudi et al., 1998; Ying et al., 2002). Thus, we reasoned that BDNF may be the factor driving the ATN response augmentation. We



tested this hypothesis with i.c.v. application of a human recombinant TrkB-Fc chimera (T 8694; Sigma-Aldrich) (5 $\mu\text{g}/\mu\text{l}$), which blocks TrkB ligand signaling (Shelton et al., 1995; Sharma et al., 2006). Stock solution was made as 250 $\mu\text{g}/\text{ml}$ in $1\times$ phosphate buffered saline (PBS) containing 0.1% bovine serum albumin (BSA) and stored at 4°C until used. TrkB-Fc or control protein (IgG, 5 $\mu\text{g}/\mu\text{l}$; I4131-10MG; Sigma-Aldrich) was injected in a 5- μl volume over a 5-min period via a Hamilton syringe in the lateral cerebral ventricle (i.c.v.). The TrkB-Fc injection was carried out immediately after the first FP recording and after 5 min (sufficient time for diffusion from the lateral cerebral ventricle into the adjacent anterior thalamic nuclei to occur) the baseline recording was continued. Under these conditions, we found a significant impairment of the pulse-dependent augmentation of the ATN FP slope (Fig. 2D, ANOVA, $F_{(1,49)} = 4.45$, $P < 0.001$, $n = 4$) and amplitude (ANOVA, $F_{(1,49)} = 2.32$, $P < 0.01$, $n = 4$, data not shown), compared to the treated with control protein (IgG, 5 $\mu\text{g}/\mu\text{l}$) group. Our results suggest a role for TrkB in this phenomenon in agreement with studies, demonstrating that blockade of BDNF-TrkB interaction by TrkB-receptor antibodies (Kang et al., 1997) or anti-BDNF antibodies (Chen et al., 1999) strongly reduces synaptic long-term potentiation LTP (Gartner et al., 2006).

The first question regarding synaptic plasticity in ATN was whether subsequent stimuli would result in synaptic facilitation or depression. These effects were examined after the baseline was stabilized and pairs of stimuli were delivered with interstimulus intervals of 20, 30, 40, 50, 100, and 250 ms. The paired-pulse (PP) ratio (Fig. 3) represents the value of the second potential (FP2) over the value of the first one (FP1) for

FIGURE 2. MTT and Dfx express different basal synaptic transmission properties. (A) Basal synaptic transmission of ATN after stimulation of MTT (white dots) and Dfx (gray dots). Averaged values of FP slope reveal gradual augmentation in the group of animals with MTT stimulation ($n = 5$) and no change throughout the 4 h recording period in the group with Dfx stimulation ($n = 5$). Even when the baseline frequency of MTT test-pulses was reduced from 0.025 Hz to 0.008 Hz (black dots) ($n = 5$), no change in the profile of the baseline occurred. The elevation was dependent on the number of the given pulses, but not on the time from the start of the experiment. The lower x-axis represents the time points of the “slow baseline” with test-pulses induced with 0.008 Hz frequency. First 180 min of the 0.008 Hz baseline are presented in the inset below left. The augmentation of the FP has slower onset when compared to the initial 180 min of the standard baseline (inset below right). Gray dashed line in the plots delineates 100% (baseline). (B) FP slope correlates differently with the initial time points of MTT baseline, depending on the given frequency; black symbols, 0.008 Hz, white symbols, 0.025 Hz. (C) Analogs represent FPs evoked at the points marked in the figures. Horizontal bar: 5 ms, vertical bar 1 mV. (D) The TrkB-Fc chimera (5 $\mu\text{g}/\mu\text{l}$) blocks the onset of field potential augmentation when applied (i.c.v.) after the first recording. A significant reduction of the FP slope is observed in TrkB-Fc-treated animals (black dots; $n = 4$) in comparison to the control protein (IgG, 5 $\mu\text{g}/\mu\text{l}$) treated group (white dots; $n = 4$).

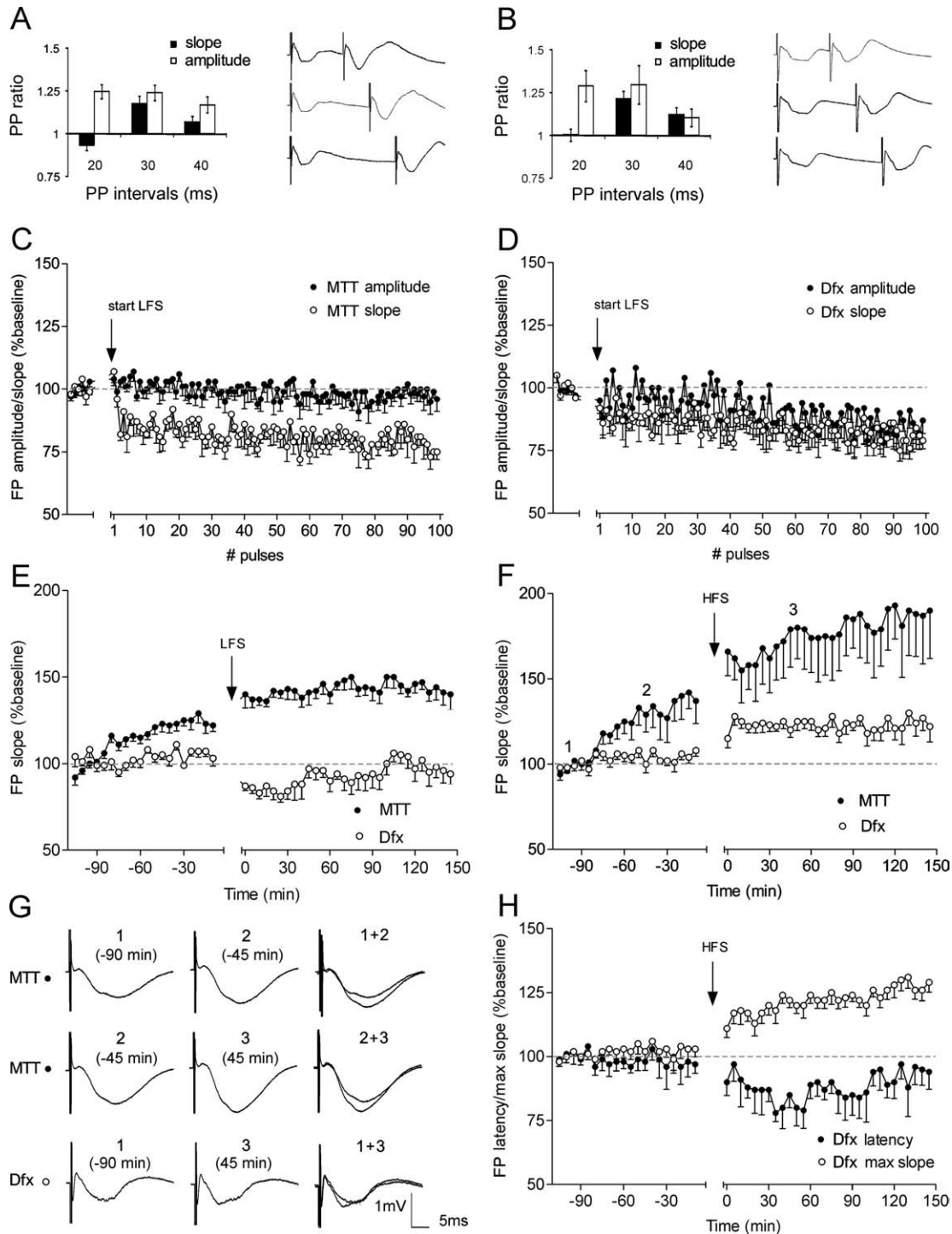


FIGURE 3. Synaptic depression and synaptic potentiation in ATN are input specific. Paired pulses lead to facilitation for mammillothalamic (A) and dorsal fornix (B) stimuli. Bars represent mean paired-pulse (PP) ratio of the second over the first response for slope (black) and amplitude (white). On the right sides are shown examples of FP traces at interstimulus intervals of 20 ms—upper pairs, 30 ms—middle pairs and 40 ms—lower pairs. (C) Analysis of the first 100 pulses of 1 Hz stimulation in the MTT-stimulated group ($n = 6$) reveals instant suppression of the FP slope (white dots) compared with the baseline period prior the start of LFS and no change of the FP amplitude (black dots). (D) The same analysis for the Dfx-stimulated group ($n = 5$) demonstrates almost parallel suppression of both FP slope (white dots) and amplitude (black dots) in the time course of 1 Hz stimulation. Gray dashed line in the plots delineates 100% (baseline). (E) 1 Hz (900 pulses) stimulation of Dfx induces LTD of the ATN FP slope in the cases with Dfx stimulation (white

dots, $n = 5$). In the group of animals with mammillothalamic recordings (black dots, $n = 7$), the same protocol failed to induce depression. (F) High-frequency stimulation (HFS) (100 Hz) leads to potent increase of the FP slope for the MTT implanted animals (black dots, $n = 5$). In contrast, no change of the slope and significant but weak potentiation of the amplitude followed the same stimulation protocol in Dfx implanted rats (white dots, $n = 7$). (G) Analogs represent FPs evoked at the points marked in the figures. Horizontal bar: 5 ms, vertical bar 1 mV. (H) Analyses of the maximal FP slope from the same data, measured by the steepest value of the negative-going potential (white dots) and FP latency, measured by the distance in ms between the initial positive deflection of the FP onset and the lowest point of the current sink (black dots) in Dfx-stimulated group ($n = 7$). HFS to ATN afferents results in an increase of the maximal slope and concurrent decrease of the field potential latency.

the slope (black bars) and the amplitude (white bars). The significance level was evaluated with post hoc Student *t*-tests by taking the average of four slope/amplitude values of FP1, for a given interval, and normalizing the average of four values for FP2 with respect to this value. Significant facilitation was present for 20, 30, and 40 ms interstimulus intervals the FP2 amplitude of the MTT-evoked responses (*t*-test, $P < 0.05$, $n = 4$) (Fig. 3A). Only the 30 ms intervals revealed significant facilitation for the MTT-evoked FP2 slope (*t*-test, $P < 0.05$), whereas the 20 ms interval evoked tendency of depression (Fig. 3A). Similarly, Dfx paired-pulses induced facilitation for 20 and 30 ms intervals for the FP2 amplitude (*t*-test, $P < 0.05$, $n = 4$) and 30 ms interval for the FP2 slope (*t*-test, $P < 0.05$) (Fig. 3B). Our next step was the exploration prolonged forms of plasticity in ATN.

To examine whether low-frequency stimulation (LFS) can induce plasticity of ATN field responses, we used a stimulation protocol known to evoke LTD. Baseline responses were collected for 30 min before the application of an LFS protocol consisting of 900 pulses at a frequency of 1 Hz. The stimulus amplitude was the same as that used for previous recordings. Stimulation of Dfx and MTT resulted in very different changes.

To address the manner in which the short-term component of LFS-induced plasticity predicts the long-term profile in both pathways, we compared the FP alterations occurring immediately after the first pulses in the time course of the 1Hz stimulation. Separate pathways have recently been shown to possess different types of short-term plasticity in the same hippocampal region in vivo (Klausnitzer and Manahan-Vaughan, 2008). While mossy fiber-CA3 synapses respond to 1Hz LFS with a potent facilitation, the commissural/associational CA3 synapses are unaffected by the same stimulation protocol (Klausnitzer and Manahan-Vaughan, 2008). In line with these findings, we compared short-term alterations in ATN responses mediated by low frequency MTT and Dfx stimulation. The transition from 0.025 Hz to 1 Hz resulted in immediate changes of the field potential for both groups. The similarity was apparent by the instant depression of FP slope for MTT (Fig. 3C), as for Dfx input (Fig. 3D) with no significant difference between the values of both groups (ANOVA, $F_{(1,105)} = 1.032$, $P = 0.17$, $n = 5$ for Dfx group and $n = 6$ for MTT). However, MTT stimulation did not affect FP amplitude (Fig. 3C), while Dfx stimuli induced a gradually developing decrease of the ATN response (Fig. 3D). Repeated measures of the first 100 pulses of the amplitude values showed significant differences between both groups (ANOVA, $F_{(1,105)} = 3.109$, $P < 0.01$, $n = 5$ for Dfx group and $n = 6$ for MTT group). LFS of Dfx induced immediate depression of FP slope compared with baseline, which continued through the 4 h recording session for the occurrence of stable LTD (Fig. 3E, ANOVA, $F_{(1,49)} = 7.24$, $P < 0.001$, $n = 5$). In the group of animals where the FP amplitude was measured after MTT stimulation, the same LFS protocol failed to induce LTD (Fig. 3E, $n = 7$) in comparison to the nonstimulated group. Analysis comparing the poststimulation values for the LFS group to the last six time points of the baseline

before the stimulation protocol reveals potentiation of the evoked response (Fig. 3E, ANOVA, $F_{(1,49)} = 5.15$, $P < 0.05$, $n = 7$). In order to increase the precision of plasticity detection and to decrease the effect of baseline pulse-dependent augmentation in MTT recordings, we timed the baseline recording for 120 min, enough for the FP values to reach a stable plateau.

The large amplitude long-term synaptic modification known as LTP (Larson and Lynch, 1986; Buzsáki et al., 1987) was the next target of our hippocampodiencephalic investigation. High frequency stimulation (HFS) consisted of 10 bursts, with each burst containing 10 pulses at 100 Hz, with an interburst interval of 10 s. After 120 min of baseline recording, a HFS was applied to the MTT in one group, and to Dfx in a second group. For the MTT-stimulated group the poststimulation recordings showed a prominent and long-lasting increase of about 160% for FP slope (Fig. 3F, ANOVA, $F_{(1,49)} = 4.02$, $P < 0.01$, $n = 5$) and for FP amplitude (ANOVA, $F_{(1,49)} = 3.70$, $P < 0.01$, $n = 5$, data not shown) compared with the last six baseline time points. When the data were compared with the nonstimulated baseline group, in which the pulse-dependent elevation of the FP parameters reached about 125% (Fig. 2A), the HFS-induced potentiation appeared as an additional level of synaptic strength increase (FP amplitude: ANOVA, $F_{(1,49)} = 4.16$, $P < 0.01$, $n = 5$; FP slope: ANOVA, $F_{(1,49)} = 4.37$, $P < 0.01$, $n = 5$). The Dfx-stimulated group demonstrated a restricted post-tetanic plasticity. No detectable change in the FP amplitude occurred ANOVA, $F_{(1,49)} = 1.22$, $P = 0.11$, $n = 7$, data not shown) while a small but significant increase in the FP slope was evident (Fig. 3F,G, ANOVA, $F_{(1,49)} = 2.09$, $P < 0.05$, $n = 7$). The dissociation between these two parameters of the FP raises a question concerning the degree to which the different components of LTP are involved (Bliss and Lomo, 1973). In order to present the HFS-induced alterations of all FP parameters, we measured the maximal slope of the FP, as defined by the steepest deviation of the pulse-evoked negative potential. Concurrently, we analyzed the latency of the FP negative peak measured in milliseconds from the FP positive onset. HFS to Dfx evoked an increase of the maximal slope (Fig. 3H, ANOVA, $F_{(1,49)} = 5.12$, $P < 0.01$, $n = 7$) as well as a significant decrease of the FP latency (Fig. 3F, ANOVA, $F_{(1,49)} = 2.47$, $P < 0.05$, $n = 7$). Both results suggest that the tetanic stimulation might affect the excitability of the recorded neuronal population, a phenomenon described in hippocampal recordings (Andersen et al., 1980).

The present study reports, for the first time, that the anterior thalamic nuclei (ATN) are capable of long-term synaptic modification of their responses. This finding corroborates the idea that, far from being a passive receiver, the anterior thalamus plays an active role in amplifying the convergence of hippocampal and mammillary body inputs (Vann and Aggleton, 2004). Furthermore, we distinguished differing and specific short- and long-term plasticity properties for the direct and the indirect pathways.

Spatial deficits after mammillary body damage are not as severe as those found after hippocampectomy (Thompson, 1981), and are typically less severe than those associated with

anterior thalamic damage (Aggleton et al., 1995; Gaffan et al., 2001). The implication is that both the direct subicular— anterior thalamic pathway and the mammillary body— anterior thalamic pathway (which presumably involves indirect subicular influences) support memory processes. The present study, therefore, set out to compare the electrophysiological properties of the two major convergent routes upon the anterior thalamic nuclei (fornix vs. mammillothalamic tract). We found that the plasticity characteristics of both pathways express a tendency to oppose each other. While HFS of mammillothalamic pathway induces large-amplitude, stable LTP of FP slope and amplitude, the direct hippocampothalamic field plasticity after HFS is expressed only with a small amplitude increase of the intrinsic excitability, measured by FP slope. LFS to mammillothalamic tract did not evoke depression of the ATN response, while the same low-frequency protocol to the dorsal fornix was followed by a long-lasting and stable depression of both FP slope and amplitude. These results favor the role of the MMB as an input that elevates the polarity of ATN plasticity, which is concurrently lowered by the direct subicularthalamic input. Inputs from the MMB are also known to target inhibitory interneurons within the anterior thalamus (Wang et al., 1999), suggesting that the activation of GABAergic synapses could affect the shape of field response. Because the fiber density of MTT and Dfx might differ and this could bias the FP representation of the degree of synaptic activation via each input, we normalized the stimulus intensity for each pathway by recording with 40% of the maximum FP amplitude that can be evoked by the afferents activation. This approach has allowed the comparison of synaptic plasticity occurring in other structures with parallel inputs (Doyere et al., 1997; Kosub et al., 2005).

Furthermore, we have detected a use-dependent plasticity of mammillothalamic synapses, which is BDNF-dependent. The detected augmentation of baseline recordings was pulse-, but not timing-dependent. This finding is consistent with a recent observation in freely moving rats that sensory thalamocortical synaptic transmission undergoes potentiation mediated by TrkB receptors (Tsanov and Manahan-Vaughan, 2007b). The long-term response to 900 pulses delivered with rate of 1 Hz suggests that MTT responses are not obeying the common model of plasticity, but rather follow a frequency-dependent activation. In addition to the opposing long-term synaptic effects of the hippocampothalamic and mammillothalamic connections, these two pathways also differ in their short-term plasticity properties. Several findings have demonstrated that different hippocampal regions respond dissimilarly to the change of test-pulses frequency from baseline to 1 Hz and these responses reflect the type of plasticity that each region expresses (Salin et al., 1996; Klausnitzer and Manahan-Vaughan, 2008). Pulses delivered with a frequency of 1 Hz induce immediate frequency depression of FP slope and amplitude of the fornix impulses that bypass the MMB. Interestingly, the same low-frequency stimulation fails to evoke frequency decrease of mammillothalamic synaptic weights. Short-term synaptic plasticity, in particular synaptic suppression, is an important component of the nonlinear temporal dynamics that lead to enhancement of neuronal

responses (Chance et al., 1998) and an increase in the signal-to-noise (S/N) ratio in neuronal processing (Abbott et al., 1997). We conclude that the rapid depression plasticity in the hippocampodiencephalic circuit is mediated by the anatomically shortest pathway—via the direct fornix projections to thalamus. Our data support and extend previous findings that reveal synaptic plasticity as one of the major properties underlying thalamic function in the adult brain (Rauschecker, 1998).

REFERENCES

- Abbott LF, Varela JA, Sen K, Nelson SB. 1997. Synaptic depression and cortical gain control. *Science* 275:220–224.
- Aggleton JP, Brown MW. 1999. Episodic memory, amnesia, and the hippocampal-anterior thalamic axis. *Behav Brain Sci* 22:425–444.
- Aggleton JP, Desimone R, Mishkin M. 1986. The origin, course, and termination of the hippocampothalamic projections in the macaque. *J Comp Neurol* 243:409–421.
- Aggleton JP, Neave N, Nagle S, Hunt PR. 1995. A comparison of the effects of anterior thalamic, mamillary body and fornix lesions on reinforced spatial alternation. *Behav Brain Res* 68:91–101.
- Akaneya Y, Tsumoto T, Kinoshita S, Hatanaka H. 1997. Brain-derived neurotrophic factor enhances long-term potentiation in rat visual cortex. *J Neurosci* 17:6707–6716.
- Andersen P, Sundberg SH, Sveen O, Swann JW, Wigstrom H. 1980. Possible mechanisms for long-lasting potentiation of synaptic transmission in hippocampal slices from guinea-pigs. *J Physiol* 302:463–482.
- Bienenstock EL, Cooper LN, Munro PW. 1982. Theory for the development of neuron selectivity: Orientation specificity and binocular interaction in visual cortex. *J Neurosci* 2:32–48.
- Bliss TVP, Lomo T. 1973. Long-lasting potentiation of synaptic transmission in the dentate area of the anesthetized rabbit following stimulation of the perforant path. *J Physiol* 232:331–356.
- Buzsáki G, Haas HL, Anderson EG. 1987. Long-term potentiation induced by physiologically relevant stimulus patterns. *Brain Res* 435:331–333.
- Chance FS, Nelson SB, Abbott LF. 1998. Synaptic depression and the temporal response characteristics of V1 cells. *J Neurosci* 18:4785–4799.
- Chen G, Kolbeck R, Barde YA, Bonhoeffer T, Kossel A. 1999. Relative contribution of endogenous neurotrophins in hippocampal long-term potentiation. *J Neurosci* 19:7983–7990.
- Conner JM, Lauterborn JC, Yan Q, Gall CM, Varon S. 1997. Distribution of brain-derived neurotrophic factor (BDNF) protein and mRNA in the normal adult rat CNS: Evidence for anterograde axonal transport. *J Neurosci* 17:2295–2313.
- Doyere V, Srebro B, Laroche S. 1997. Heterosynaptic LTD, depotentiation in the medial perforant path of the dentate gyrus in the freely moving rat. *J Neurophysiol* 77:571–578.
- Gaffan EA, Bannerman DM, Warburton EC, Aggleton JP. 2001. Rats' processing of visual scenes: Effects of lesions to fornix, anterior thalamus, mamillary nuclei or the retrohippocampal region. *Behav Brain Res* 121:103–117.
- Gartner A, Polnau DG, Staiger V, Sciarretta C, Minichiello L, Thoenen H, Bonhoeffer T, Korte M. 2006. Hippocampal long-term potentiation is supported by presynaptic and postsynaptic tyrosine receptor kinase B-mediated phospholipase C gamma signaling. *J Neurosci* 26:3496–3504.
- Ishizuka N. 2001. Laminar organization of the pyramidal cell layer of the subiculum in the rat. *J Comp Neurol* 435:89–110.

- Kang H, Schuman EM. 1995. Long-lasting neurotrophin-induced enhancement of synaptic transmission in the adult hippocampus. *Science* 267:1658–1662.
- Kang H, Welcher AA, Shelton D, Schuman EM. 1997. Neurotrophins and time: Different roles for TrkB signaling in hippocampal long-term potentiation. *Neuron* 19:653–664.
- Klausnitzer J, Manahan-Vaughan D. 2008. Frequency facilitation at mossy fiber-CA3 synapses of freely behaving rats is regulated by adenosine A1 receptors. *J Neurosci* 28:4836–4840.
- Kosub KA, Do VH, Derrick BE. 2005. NMDA receptor antagonists block heterosynaptic long-term depression (LTD) but not long-term potentiation (LTP) in the CA3 region following lateral perforant path stimulation. *Neurosci Lett* 374:29–34.
- Kruger L, Saporta S, Swanson LW. 1995. *Photographic Atlas of the Rat Brain: The Cell and Fiber Architecture Illustrated in Three Planes with Stereotaxic Coordinates*. New York: Cambridge University Press. 299 pp.
- Larson J, Lynch G. 1986. Induction of synaptic potentiation in the hippocampus by patterned stimulation involves two events. *Science* 232:985–988.
- Lisman JE. 1994. The CaM-kinase hypothesis for the storage of synaptic memory. *Trends Neurosci* 17:406–412.
- Madison DV, Malenka RC, Nicoll RA. 1991. Mechanisms underlying long-term potentiation of synaptic transmission. *Annu Rev Neurosci* 14:379–397.
- Meibach RC, Siegel A. 1975. The origin of fornix fibers which project to the mammillary bodies in the rat: A horseradish peroxidase study. *Brain Res* 88:508–512.
- Messaoudi E, Bardsen K, Srebro B, Bramham CR. 1998. Acute intra-hippocampal infusion of BDNF induces lasting potentiation of synaptic transmission in the rat dentate gyrus. *J Neurophysiol* 79:496–499.
- Moser EI, Krobot KA, Moser MB, Morris RG. 1998. Impaired spatial learning after saturation of long-term potentiation. *Science* 281:2038–2042.
- Rauschecker JP. 1998. Cortical control of the thalamus: Top-down processing and plasticity. *Nat Neurosci* 1:179–180.
- Salin PA, Scanziani M, Malenka RC, Nicoll RA. 1996. Distinct short-term plasticity at two excitatory synapses in the hippocampus. *Proc Natl Acad Sci USA* 93:13304–13309.
- Sharma SK, Sherff CM, Stough S, Hsuan V, Carew TJ. 2006. A tropomyosin-related kinase B ligand is required for ERK activation, long-term synaptic facilitation, and long-term memory in aplysia. *Proc Natl Acad Sci USA* 103:14206–14210.
- Shelton DL, Sutherland J, Gripp J, Camerato T, Armanini MP, Phillips HS, Carroll K, Spencer SD, Levinson AD. 1995. Human trks: Molecular cloning, tissue distribution, and expression of extracellular domain immunoadhesins. *J Neurosci* 15:477–491.
- Snyder SE, Li J, Salton SR. 1997. Comparison of VGF, trk mRNA distributions in the developing and adult rat nervous systems. *Brain Res Mol Brain Res* 49:307–311.
- Thompson R. 1981. Rapid forgetting of a spatial habit in rats with hippocampal lesions. *Science* 212:959–960.
- Tsanov M, Manahan-Vaughan D. 2007a. The adult visual cortex expresses dynamic synaptic plasticity that is driven by the light-dark cycle. *J Neurosci* 27:8414–8421.
- Tsanov M, Manahan-Vaughan D. 2007b. Intrinsic, light-independent and visual-activity dependent mechanisms cooperate in the shaping of the field response in rat visual cortex. *J Neurosci* 27:8422–8429.
- Van der Werf YD, Scheltens P, Lindeboom J, Witter MP, Uylings HB, Jolles J. 2003. Deficits of memory, executive functioning and attention following infarction in the thalamus; a study of 22 cases with localised lesions. *Neuropsychologia* 41:1330–1344.
- Vann SD, Aggleton JP. 2004. The mammillary bodies: Two memory systems in one? *Nat Rev Neurosci* 5:35–44.
- von Cramon DY, Hebel N, Schuri U. 1985. A contribution to the anatomical basis of thalamic amnesia. *Brain* 108:993–1008.
- Wang B, Gonzalo-Ruiz A, Sanz JM, Campbell G, Lieberman AR. 1999. Immunoelectron microscopic study of gamma-aminobutyric acid inputs to identified thalamocortical projection neurons in the anterior thalamus of the rat. *Exp Brain Res* 126:369–382.
- Warburton EC, Baird A, Morgan A, Muir JL, Aggleton JP. 2001. The conjoint importance of the hippocampus and anterior thalamic nuclei for allocentric spatial learning: Evidence from a disconnection study in the rat. *J Neurosci* 21:7323–7330.
- Ying SW, Futter M, Rosenblum K, Webber MJ, Hunt SP, Bliss TV, Bramham CR. 2002. Brain-derived neurotrophic factor induces long-term potentiation in intact adult hippocampus: Requirement for ERK activation coupled to CREB and upregulation of Arc synthesis. *J Neurosci* 22:1532–1540.